AMERICAN SOCIETY FOR MICROBIOLOGY | Journal of Virology®

VIRUS-CELL INTERACTIONS

A Conserved Mechanism of APOBEC3 Relocalization by Herpesviral Ribonucleotide Reductase Large Subunits

Adam Z. Cheng,[a,b,c,d] Sofia N. Moraes,[a,b,c,d] Claire Attarian,[a,b,c,d] Jaime Yockteng-Melgar,[e,f] Matthew C. Jarvis,[a,b,c,d] Matteo Biolatti,[g] Ganna Galitska,[g] Valentina Dell'Oste,[g] Lori Frappier,[e] Craig J. Bierle,[c,h] Stephen A. Rice,[c,i] Reuben S. Harris[a,b,c,d,j]

[a]Department of Biochemistry, Molecular Biology and Biophysics, University of Minnesota, Minneapolis, Minnesota, USA
[b]Masonic Cancer Center, University of Minnesota, Minneapolis, Minnesota, USA
[c]Institute for Molecular Virology, University of Minnesota, Minneapolis, Minnesota, USA
[d]Center for Genome Engineering, University of Minnesota, Minneapolis, Minnesota, USA
[e]Department of Molecular Genetics, University of Toronto, Toronto, Ontario, Canada
[f]Facultad de Ciencias de la Vida, Escuela Superior Politécnica del Litoral, Guayaquil, Ecuador
[g]Laboratory of Pathogenesis of Viral Infections, Department of Public Health and Pediatric Sciences, University of Turin, Turin, Italy
[h]Department of Pediatrics, Division of Pediatric Infectious Diseases and Immunology, University of Minnesota, Minneapolis, Minnesota, USA
[i]Department of Microbiology and Immunology, University of Minnesota, Minneapolis, Minnesota, USA
[j]Howard Hughes Medical Institute, University of Minnesota, Minneapolis, Minnesota, USA

ABSTRACT An integral part of the antiviral innate immune response is the APOBEC3 family of single-stranded DNA cytosine deaminases, which inhibits virus replication through deamination-dependent and -independent activities. Viruses have evolved mechanisms to counteract these enzymes, such as HIV-1 Vif-mediated formation of a ubiquitin ligase to degrade virus-restrictive APOBEC3 enzymes. A new example is Epstein-Barr virus (EBV) ribonucleotide reductase (RNR)-mediated inhibition of cellular APOBEC3B (A3B). The large subunit of the viral RNR, BORF2, causes A3B relocalization from the nucleus to cytoplasmic bodies and thereby protects viral DNA during lytic replication. Here, we use coimmunoprecipitation and immunofluorescence microscopy approaches to ask whether this mechanism is shared with the closely related gammaherpesvirus Kaposi's sarcoma-associated herpesvirus (KSHV) and the more distantly related alphaherpesvirus herpes simplex virus 1 (HSV-1). The large RNR subunit of KSHV, open reading frame 61 (ORF61), coprecipitated multiple APOBEC3s, including A3B and APOBEC3A (A3A). KSHV ORF61 also caused relocalization of these two enzymes to perinuclear bodies (A3B) and to oblong cytoplasmic structures (A3A). The large RNR subunit of HSV-1, ICP6, also coprecipitated A3B and A3A and was sufficient to promote the relocalization of these enzymes from nuclear to cytoplasmic compartments. HSV-1 infection caused similar relocalization phenotypes that required ICP6. However, unlike the infectivity defects previously reported for BORF2-null EBV, ICP6 mutant HSV-1 showed normal growth rates and plaque phenotypes. Combined, these results indicate that both gamma- and alphaherpesviruses use a conserved RNR-dependent mechanism to relocalize A3B and A3A and furthermore suggest that HSV-1 possesses at least one additional mechanism to neutralize these antiviral enzymes.

IMPORTANCE The APOBEC3 family of DNA cytosine deaminases constitutes a vital innate immune defense against a range of different viruses. A novel counterrestriction mechanism has recently been uncovered for the gammaherpesvirus EBV, in which a subunit of the viral protein known to produce DNA building blocks (ribonucleotide reductase) causes A3B to relocalize from the nucleus to the cytosol. Here, we extend these observations with A3B to include a closely related gammaherpesvirus, KSHV, and a more distantly related alphaherpesvirus, HSV-1. These different viral

Citation Cheng AZ, Moraes SN, Attarian C, Yockteng-Melgar J, Jarvis MC, Biolatti M, Galitska G, Dell'Oste V, Frappier L, Bierle CJ, Rice SA, Harris RS. 2019. A conserved mechanism of APOBEC3 relocalization by herpesviral ribonucleotide reductase large subunits. J Virol 93:e01539-19. https://doi.org/10.1128/JVI.01539-19.

Editor Viviana Simon, Icahn School of Medicine at Mount Sinai

Address correspondence to Reuben S. Harris, rsh@umn.edu.

Received 9 September 2019
Accepted 17 September 2019
Accepted manuscript posted online 18 September 2019
Published 13 November 2019

ribonucleotide reductases also caused relocalization of A3A, which is 92% identical to A3B. These studies are important because they suggest a conserved mechanism of APOBEC3 evasion by large double-stranded DNA herpesviruses. Strategies to block this host-pathogen interaction may be effective for treating infections caused by these herpesviruses.

KEYWORDS APOBEC3A, APOBEC3B, innate antiviral immunity, herpesviruses, ribonucleotide reductase

An important arm of the innate immune response lies in the APOBEC family of single-stranded DNA cytosine deaminases (1–3). Each of the seven human APOBEC3 (A3) enzymes, A3A to -D and A3F to -H, have been implicated in the restriction and mutation of a variety of different human viruses, including retroviruses (HIV-1, HIV-2, and human T cell leukemia virus type 1 [HTLV-1]) (4–8), endogenous retroviruses (human endogenous retrovirus [HERV]) (9, 10), hepadnaviruses (hepatitis B virus [HBV]) (11, 12), small DNA tumor viruses (human papillomavirus [HPV] and JC/BK polyomavirus [JC/BK-PyV]) (13–17), and, most recently, the gammaherpesvirus Epstein-Barr virus (EBV) (18, 19). It is difficult, if not impossible, to predict *a priori* which subset of APOBEC3 enzymes has the potential to engage a given virus and, furthermore, how that virus might counteract potentially restrictive A3 enzymes. For instance, the lentiviruses HIV-1 and HIV-2 encode an accessory protein called Vif that heterodimerizes with the cellular transcription cofactor CBF-β (core binding factor subunit beta) and recruits a cellular ubiquitin ligase complex to trigger the degradation of restrictive A3 enzymes (20, 21).

Human herpesviruses can be grouped into three distinct subfamilies (alpha-, beta-, and gammaherpesviruses) (phylogeny is shown in Fig. 1A). Pathogenic alpha- and betaherpesviruses include herpes simplex virus 1 (HSV-1) and cytomegalovirus (CMV), respectively, and the gammaherpesvirus subfamily includes EBV and Kaposi's sarcoma-associated herpesvirus (KSHV). We recently identified an A3 counteraction mechanism for EBV (18). We demonstrated that the large subunit of the viral ribonucleotide reductase (RNR), BORF2, inhibits APOBEC3B (A3B) by directly binding and relocalizing it from the nucleus to the cytoplasmic compartment. This counteraction mechanism prevents the normally nucleus-localized A3B enzyme from deaminating viral genomic DNA cytosines to uracils during lytic replication. In the absence of BORF2, A3B inflicted C/G-to-T/A mutations in EBV genomes and reduced viral titers and infectivity. We also showed that the homologous protein from KSHV, open reading frame 61 (ORF61), is similarly capable of binding and relocalizing A3B (18).

Here, we ask whether the viral RNR-mediated A3B counteraction mechanism is specific for gammaherpesviruses or more generally acting by assessing interactions between gammaherpesvirus BORF2/ORF61 and other human A3 enzymes and by determining whether the more distantly related alphaherpesvirus HSV-1 has a similar A3 neutralization mechanism (RNR nomenclature is shown in Fig. 1A, and protein domains are depicted in Fig. 1B). We found that in addition to binding and relocalizing A3B, both BORF2 and ORF61 were also capable of coimmunoprecipitation (co-IP) and relocalization of A3A. Additionally, we found that the HSV-1 RNR large subunit, ICP6, similarly binds and relocalizes both A3B and A3A. Overexpression studies showed that ICP6 alone is sufficient for A3B and A3A relocalization. Infection studies with wild-type and mutant viruses demonstrated that ICP6 mediates this relocalization activity in the context of infected cells and that no other viral protein is capable of this relocalization function. However, despite the likely conservation of the A3B/A relocalization mechanism, the infectivity of ICP6 mutant HSV-1 was not affected by A3B or A3A, suggesting the existence of a functionally redundant A3 neutralization mechanism.

RESULTS

EBV BORF2 and KSHV ORF61 bind and relocalize both A3B and A3A. Our previous co-IP experiments indicated that EBV BORF2 interacts strongly with A3B and weakly with A3A and A3F (see Fig. 1c in reference 18). EBV BORF2 was both necessary

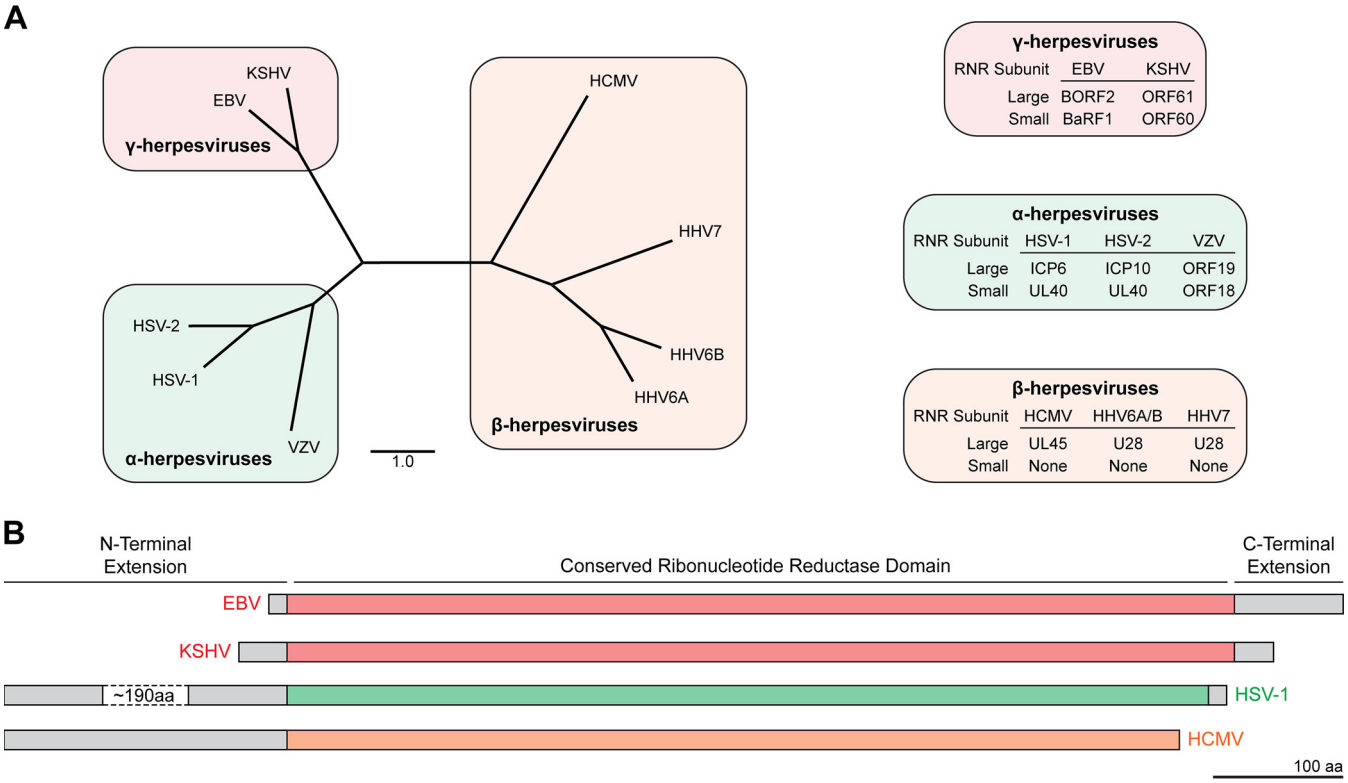

FIG 1 Herpesvirus ribonucleotide reductases conservation. (A) Amino acid sequences from ribonucleotide reductase large subunits were aligned using multiple-sequence comparison by log expectation (MUSCLE), and phylogeny was constructed using a neighbor-joining tree without distance corrections and scaled for equal branch lengths. Shaded boxes indicate herpesvirus subfamilies, which group closely to established phylogenetic trees. Protein names for human herpesvirus ribonucleotide reductase large and small subunits are shown on the right. (B) Schematic of representative RNR large subunit polypeptides from alpha-, beta-, and gammaherpesviruses with conserved core sequences (colored) and unique N- and C-terminal extensions (gray). The diagram is approximately to scale, with an ~190-amino-acid (aa) portion of HSV-1 ICP6 omitted to fit the figure.

and sufficient to relocalize A3B in a variety of different cell types, including endogenous A3B in the AGS gastric carcinoma cell line and the M81 B cell line (18). However, our original studies did not address whether EBV BORF2 could functionally interact with and relocalize any of these related human A3 enzymes. We therefore performed immunofluorescence (IF) microscopy studies of U2OS cells overexpressing A3-mCherry constructs with either an empty vector or BORF2-FLAG (Fig. 2A). As reported previously, A3B is nuclear, A3A has a cell-wide localization, A3H is cytoplasmic and nucleolar, and the other A3s are cytoplasmic (22–26). Also as expected, BORF2 caused a robust and complete relocalization of nuclear A3B to perinuclear aggregates. Interestingly, BORF2 coexpression with A3A led to the presence of novel linear elongated structures concomitant with normal A3A localization. The localization patterns of the other five A3s were unchanged by BORF2 coexpression. Small BORF2 punctate structures were also noted under all conditions, including the mCherry control, which is likely due to transfected BORF2 interacting with endogenous A3B (previously shown to be elevated in U2OS cells [18]). Similar A3B and A3A relocalization patterns were evident in Vero cells, except that A3A was relocalized throughout the whole cell, without elongated structures (Fig. 2B and data not shown).

Like EBV BORF2, KSHV ORF61 was also shown to coimmunoprecipitate and relocalize A3B (18). However, our original studies did not examine the specificity of this interaction in comparison with related human A3 enzymes. We therefore used co-IP experiments to evaluate KSHV ORF61 interactions with a full panel of human A3 enzymes. ORF61-FLAG was coexpressed with A3-hemagglutinin (HA) family members in 293T cells, subjected to anti-FLAG affinity purification, and analyzed by immunoblotting (Fig. 3A). The ORF61-FLAG pulldown resulted in A3B recovery, as described previously (18).

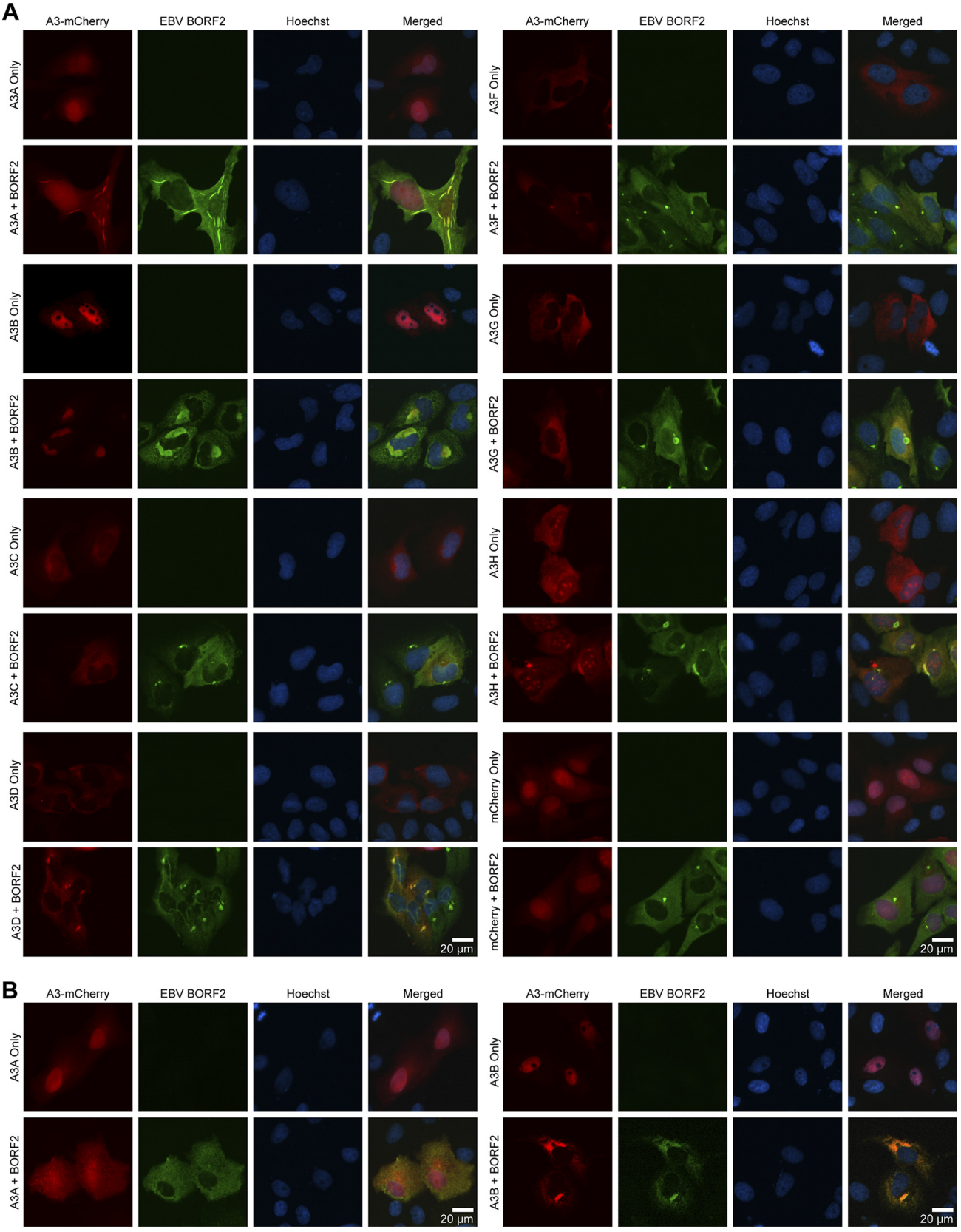

FIG 2 EBV BORF2 relocalizes A3B and A3A. (A) Representative images of U2OS cells expressing the indicated A3-mCherry constructs alone or in combination with a BORF2-FLAG construct. Cells were fixed at 48 h posttransfection, permeabilized, and stained with anti-FLAG antibody and Hoechst stain. (B) Representative images of Vero cells expressing A3A/B-mCherry alone or in combination with BORF2-FLAG. Cells were fixed at 48 h posttransfection, permeabilized, and stained with anti-FLAG antibody and Hoechst stain.

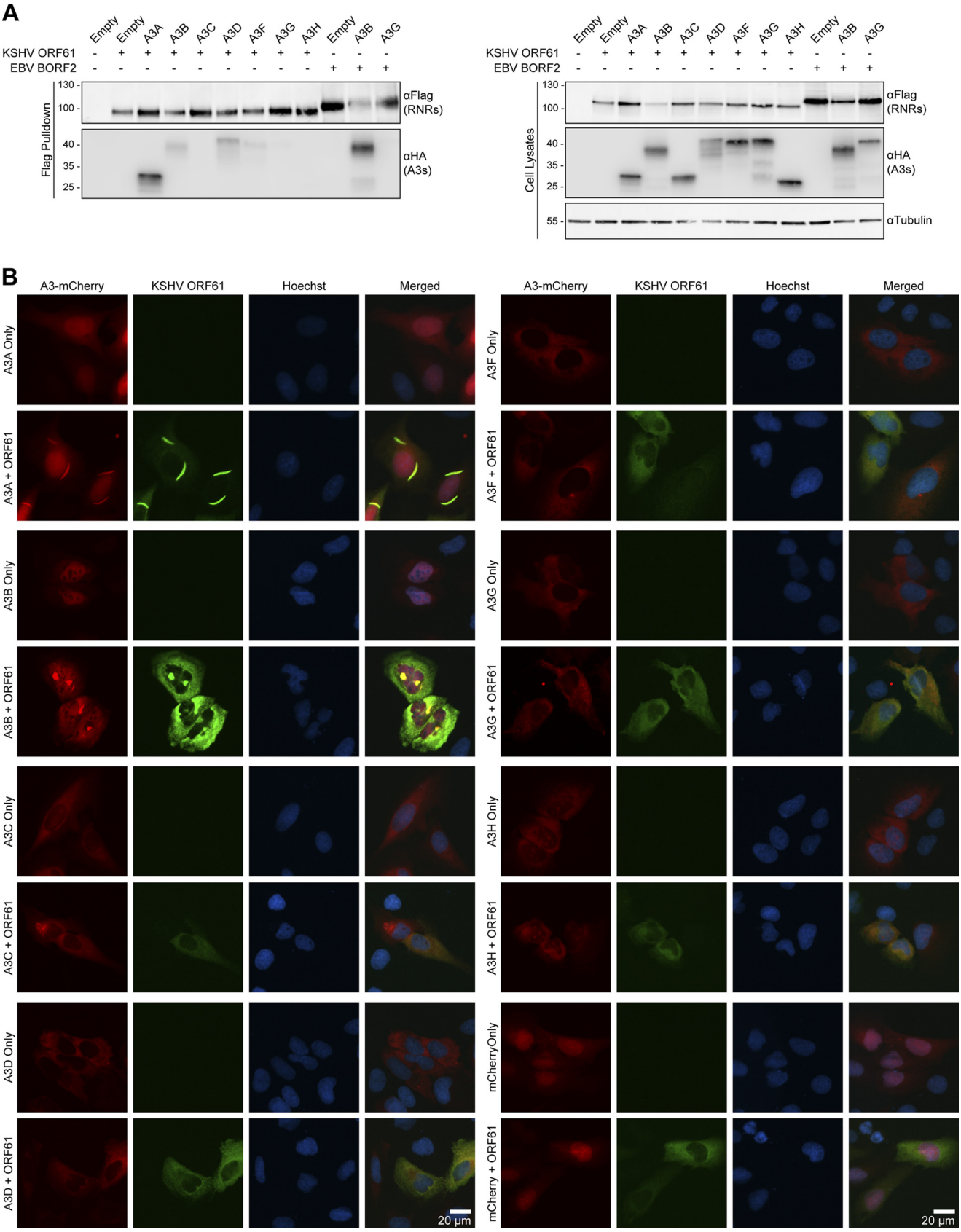

FIG 3 KSHV ORF61 relocalizes A3B and A3A. (A) Coimmunoprecipitation of transfected KSHV ORF61-FLAG with the indicated A3-HA constructs in 293T cells. Cells were lysed at 48 h posttransfection for anti-FLAG pulldown, and the resulting proteins were analyzed by immunoblotting. EBV FLAG-BORF2 transfections

(Continued on next page)

In addition, the ORF61-FLAG IP also yielded a robust interaction with A3A and weaker interactions with A3D and A3F.

These KSHV ORF61-A3 interactions were then evaluated by IF microscopy experiments to look for changes in A3 localization in U2OS cells (Fig. 3B). As expected (18), KSHV ORF61 caused A3B to relocalize to perinuclear bodies. Moreover, as described above for BORF2 and A3A, ORF61 coexpression caused a portion of the cellular A3A to localize to intense elongated linear structures in the cytosolic compartment (Fig. 3B). No other A3 proteins showed an altered subcellular localization in these experiments. Similar IF microscopy observations were made using the same constructs in HeLa cells (data not shown). Combined, these new results indicate that both A3B and A3A are cellular targets of EBV BORF2 and KSHV ORF61. The potential relevance of these interactions to the pathogenesis of these viruses is considered in Discussion.

HSV-1 ICP6 binds and relocalizes A3B and A3A. To test whether the RNR-mediated A3B/A relocalization mechanism is more broadly conserved, a series of co-IP experiments was done with the large RNR subunit of the pathogenic alphaherpesvirus HSV-1, ICP6. FLAG-ICP6 was coexpressed with each of the seven different HA-tagged human A3s in 293T cells and subjected to anti-FLAG IP as described above. The EBV BORF2-A3B interaction was used as a positive control and the BORF2-A3G interaction was used as a negative control to be able to compare the relative strengths of pulldown between RNRs and A3s. HSV-1 ICP6 showed a strong interaction with A3A and weaker, but detectable, interactions with A3B, A3C, and A3D (Fig. 4A).

Next, IF microscopy was used to assess functional interactions between HSV-1 ICP6 and each of the human A3 enzymes. Human U2OS osteosarcoma cells were cotransfected with mCherry-tagged A3s and either an empty vector or FLAG-tagged HSV-1 ICP6 and analyzed by IF after 48 h (Fig. 4B). On its own, EBV BORF2 shows a cytoplasmic distribution, and as shown above and previously (18), it was able to completely relocalize A3B from the nucleus to the cytoplasm. In comparison, HSV-1 FLAG-ICP6 showed a broadly cytoplasmic localization that did not change significantly with coexpression of any A3. However, coexpression of FLAG-ICP6 and A3B-mCherry or A3A-mCherry led to a near-complete relocalization of these DNA deaminases from the nucleus to the cytoplasm. HSV-1 ICP6 did not cause a significant relocalization of any of the other A3s. The dramatic relocalization results with A3B and A3A suggested that functionally relevant interactions may be occurring with these enzymes.

HSV-1 infection relocalizes A3B, A3A, and A3C. To address whether HSV-1 infection similarly promotes the relocalization of A3B and A3A, U2OS cells were transfected with A3-mCherry constructs 48 h prior to either mock or HSV-1 infection. We used K26GFP, an HSV-1 strain that has a green fluorescent protein (GFP) moiety fused to the capsid protein VP26 to allow the identification of infected cells (27). Cells were analyzed by IF microscopy at 8 h postinfection (hpi) (Fig. 5A). Similar to the ICP6 overexpression experiments described above, HSV-1 infection caused A3A to relocalize to the cytoplasmic compartment and caused A3B to change from a predominantly nuclear localization to a more cell-wide distribution. A3C also changed from a predominantly cytoplasmic localization to a more diffuse whole-cell distribution, whereas A3D, A3F, A3G, and A3H were unchanged by HSV-1 infection. In an independent experiment, quantification was done for the HSV-1-induced relocalization of A3A-mCherry, A3B-mCherry, and, as a representative nonaltered control, A3G-mCherry (Fig. 5B). This analysis confirmed that HSV-1 infection leads to significant changes in both A3A and A3B localizations, whereas A3G is unaffected. Similar relocalization patterns were found in HeLa cells following HSV-1 K26GFP infection (data not shown). Moreover, time course experiments showed that relocalization of A3A was detectable by as early as 3 hpi, A3B

FIG 3 Legend (Continued)
with A3B and A3G were used as positive and negative co-IP controls, respectively. (B) Representative images of U2OS cells transfected with either A3-mCherry or FLAG-RNR constructs. Cells were fixed at 48 h posttransfection, permeabilized, and stained with anti-FLAG antibody and Hoechst stain. Cotransfection with A3B-mCherry and EBV BORF2-FLAG was used as a positive control for relocalization from nuclear to cytoplasmic aggregates. A3 localization was compared in the presence and absence of KSHV ORF61-FLAG cotransfection.

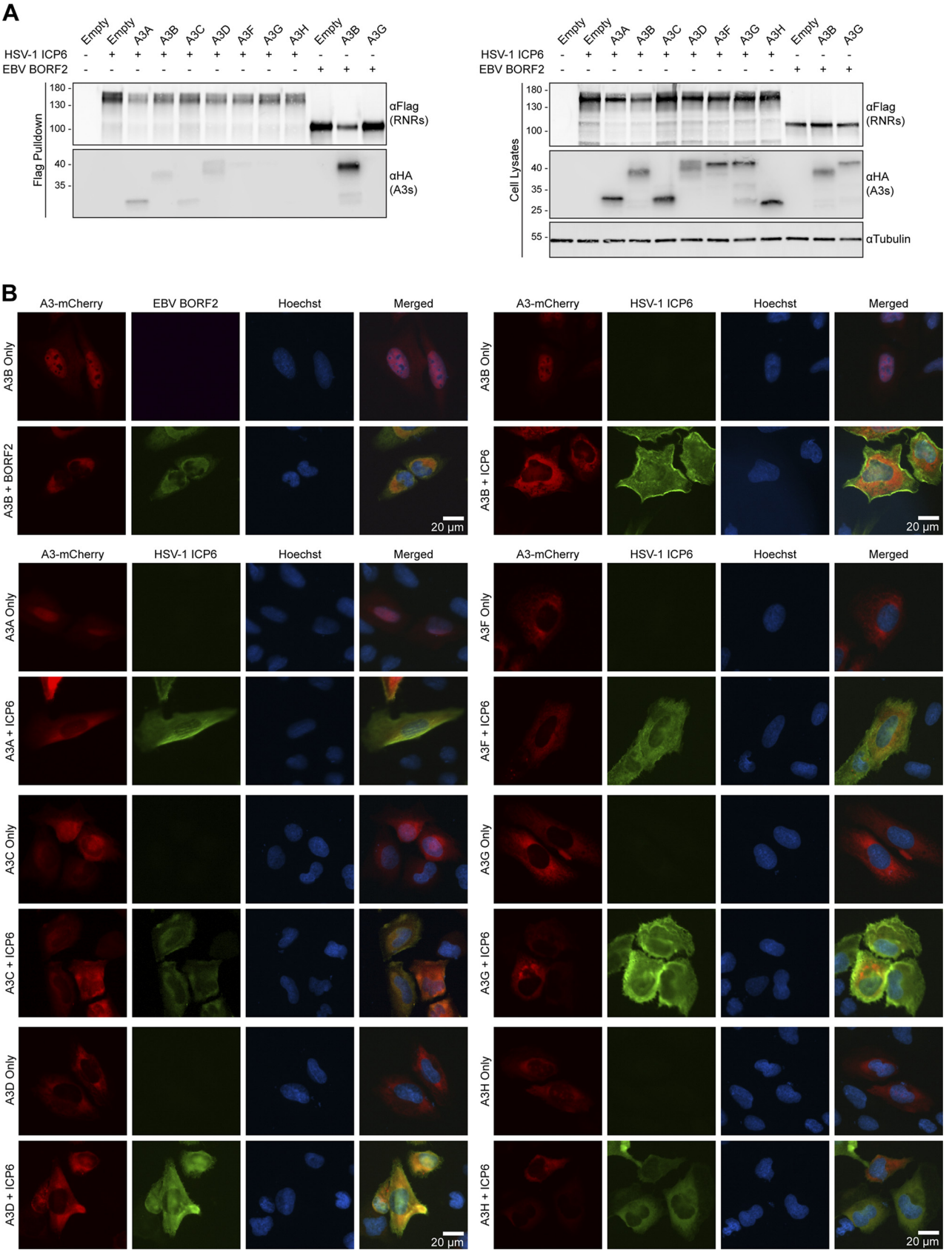

FIG 4 HSV-1 ICP6 binds and relocalizes A3B and A3A. (A) Coimmunoprecipitation of transfected HSV-1 FLAG-ICP6 with the indicated A3-HA constructs in 293T cells. Cells were lysed at 48 h posttransfection for anti-FLAG pulldown, and the resulting proteins were analyzed by immunoblotting. EBV

(Continued on next page)

and A3C relocalization became apparent by 6 or 9 hpi, and A3G was not observed to relocalize at any time point (Fig. 6 and data not shown). These kinetic differences may reflect differential affinities of the viral protein(s) for binding to these cellular A3 enzymes and/or different competitions with cellular interactors.

HSV-1-mediated relocalization of A3B and A3A requires ICP6. To investigate whether the HSV-1 large RNR subunit is required for A3A/B/C relocalization, we next examined A3 localization in cells following infection with an HSV-1 KOS1.1 strain lacking ICP6 due to a deletion of the *UL39* gene (*UL39* encodes ICP6) (28). Vero cells were transfected with A3-mCherry constructs 48 h prior to mock infection or infection with KOS1.1 or KOSΔICP6. After 8 h, cells were fixed, permeabilized, and subjected to IF analysis by staining for the HSV-1 immediate early protein ICP27 to mark infected cells and monitoring A3 localization through mCherry fluorescence. As described above, HSV-1 infection caused the relocalization of A3A, A3B, and A3C (Fig. 7A). However, only the relocalization A3A and A3B was ICP6 dependent, whereas A3C redistributed regardless of the presence of ICP6. Quantification of A3A and A3B relocalization showed that these proteins were not significantly changed upon KOS1.1ΔICP6 infection compared to mock-infected cells (Fig. 5B). These results provide strong support for the mechanistic conservation of the RNR large subunit interaction with A3A and A3B and also indicate that A3C relocalization by HSV-1 is mechanistically distinct.

To further investigate the role of ICP6 in mediating A3A and A3B relocalization, U2OS cells were infected with an HSV-1 KOS mutant with a deletion in the *ICP4* gene (29). ICP4, an immediate early protein, is the major transcriptional activator protein of HSV-1 (29). *ICP4*-null mutants exhibit a strict block of the expression of nearly all viral delayed-early and late genes but are competent to express the viral immediate early genes (*ICP0*, *ICP22*, *UL54*, and *US12*) as well as the *UL39* gene, a delayed-early gene that is uniquely transactivated by ICP0 (30). In fact, at intermediate and late times postinfection, *ICP4*-null mutants express abnormally high levels of these immediate early proteins as well as ICP6 (29). Similar to what was seen for wild-type HSV-1 infection, infection with the HSV-1 KOSΔICP4 mutant also led to A3A and A3B relocalization but with noticeably more pronounced phenotypes (Fig. 7B; also see Fig. 5B for quantification of data from an independent experiment). For instance, this mutant virus caused A3B-mCherry to form perinuclear aggregates reminiscent of previously observed BORF2-A3B bodies (18) (Fig. 7B). Interestingly, A3C localization became predominantly nuclear upon HSV-1 KOSΔICP4 infection, suggesting that one of the other four immediate early proteins besides ICP4 induces its relocalization. Taken together, these data show that HSV-1 ICP6 is both necessary and sufficient for the relocalization of A3A and A3B and that at least one other viral factor is responsible for A3C relocalization. Identification of this factor will be the subject of a future investigation.

Effect of A3B and A3A on HSV-1 replication. We next sought to test the effect of A3 expression on HSV-1 replication, with or without ICP6. HFF-1 cells were stably transduced to express HA-tagged A3 constructs and then infected at a low multiplicity of infection (MOI) (0.001 PFU/cell) with wild-type HSV-1 KOS1.1 or KOSΔICP6. At 48 hpi, the cultures were harvested, and after freeze-thawing to release infectious progeny, the titers were determined on Vero cells to compare levels of virus production. As previously described, KOSΔICP6 exhibited a 1- to 2-log defect in virus replication compared to wild-type KOS (28). However, there was no significant difference in either KOS1.1 or KOSΔICP6 virus titers produced from control HFF-1 cells or HFF-1 cells expressing different A3 family members (Fig. 8A).

To further test whether A3B or A3A can restrict HSV-1 replication, we performed plaque assays on U2OS and Vero cells stably transduced with HA-tagged A3 constructs.

FIG 4 Legend (Continued)
FLAG-BORF2 transfections with A3B and A3G were used as positive and negative co-IP controls, respectively. (B) Representative images of U2OS cells transfected with either A3-mCherry or FLAG-RNR constructs. Cells were fixed at 48 h posttransfection, permeabilized, and stained with anti-FLAG antibody and Hoechst stain. Cotransfection with A3B-mCherry and EBV FLAG-BORF2 was used as the positive control for relocalization from nuclear to cytoplasmic aggregates. A3 localization was compared in the presence and absence of HSV-1 FLAG-ICP6 cotransfection.

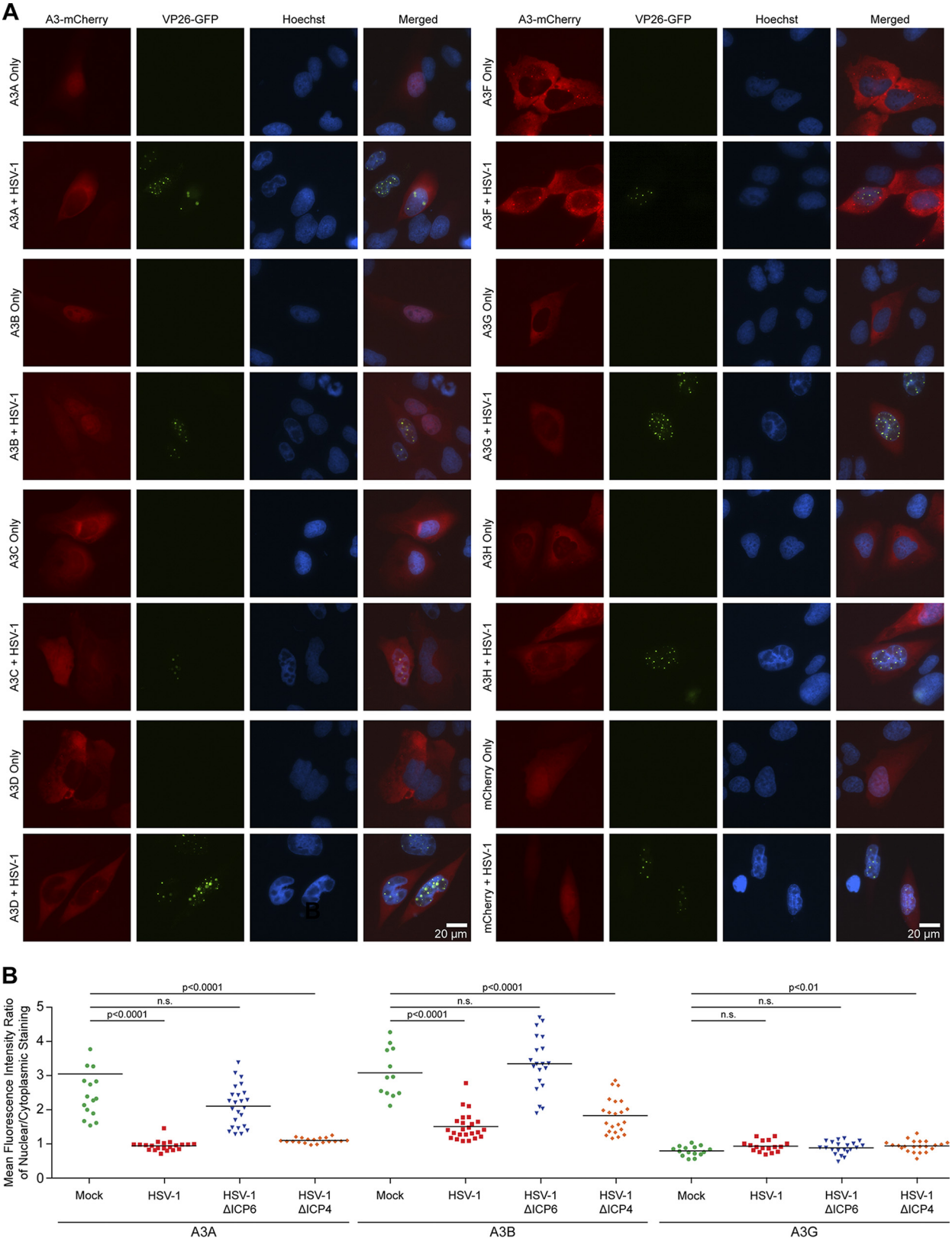

FIG 5 HSV-1 infection relocalizes A3B and A3A. (A) Representative images of U2OS cells transfected with A3-mCherry constructs, followed by mock or HSV-1 K26GFP infection at 48 h posttransfection. Cells were fixed at 8 hpi, stained with Hoechst stain, and then imaged directly. The viral capsid protein VP26 is tagged with GFP, which marks infected cells. (B) Quantification of A3 localization patterns in U2OS cells after mock infection or infection with different HSV-1 strains. The mean fluorescence intensity of the nuclear signal was divided by that of the cytoplasmic compartment. Statistical analysis was performed using unpaired Student's *t* test between the indicated groups (n.s., not significant [$P > 0.01$]).

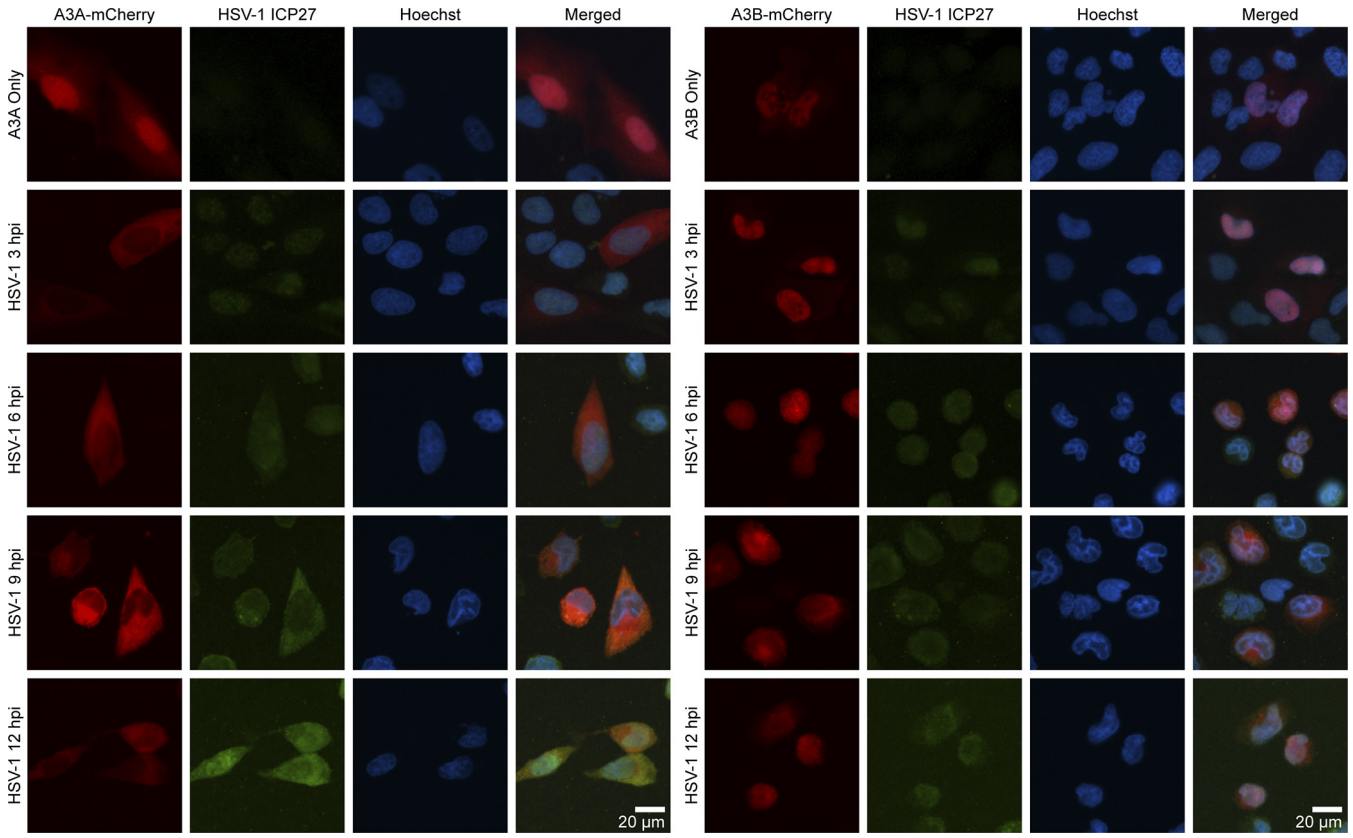

FIG 6 Time course of HSV-1-mediated relocalization of A3B and A3A. Shown are representative images of U2OS cells transfected with A3-mCherry constructs, followed by mock or HSV-1 KOS1.1 infection at 48 h posttransfection. Cells were fixed at either 3, 6, 9, or 12 hpi and stained with anti-ICP27 antibody to mark infected cells and Hoechst stain to stain the nuclear compartment.

Confluent monolayers were incubated with serial dilutions of KOS1.1 or KOSΔICP6 and incubated for 3 days to allow plaque formation. However, expression of A3A or A3B did not have a discernible effect on the number or size of KOS1.1 or KOSΔICP6 plaques (Fig. 8B). These data suggest that even without ICP6, HSV-1 is not readily susceptible to restriction by A3A or A3B, possibly because it possesses other defenses against these virus restriction factors.

DISCUSSION

We previously described a novel mechanism for A3B counteraction by the gammaherpesvirus RNR large subunits, EBV BORF2 and KSHV ORF61 (18). These viral proteins interact directly with A3B, inhibit its DNA deaminase activity, and relocalize it from the nuclear to the cytoplasmic compartment. The importance of this A3B counteraction mechanism is evidenced by BORF2-null EBV eliciting lower viral titers, decreased infectivity, and an accumulation of A3B signature C/G-to-T/A mutations. Here, we investigated the question of specificity by comparing interactions with the full repertoire of seven different human A3 enzymes, and we also addressed the potential for broader conservation by asking whether the alphaherpesvirus HSV-1 possesses a similar APOBEC3 relocalization mechanism. Although EBV BORF2 and KSHV ORF61 were able to interact with several different A3 proteins in co-IP experiments, these viral RNR large subunits promoted the relocalization of only A3B and A3A. HSV-1 ICP6 showed a similarly broad range of co-IP interactions but also promoted the relocalization of only A3B and A3A. Wild-type but not ICP6 deletion mutant HSV-1 infections yielded similar A3B and A3A relocalization phenotypes. Combined, data from these studies indicate that human gamma- and alphaherpesviruses possess a conserved A3B/A relocalization mechanism mediated by the viral RNR large subunit.

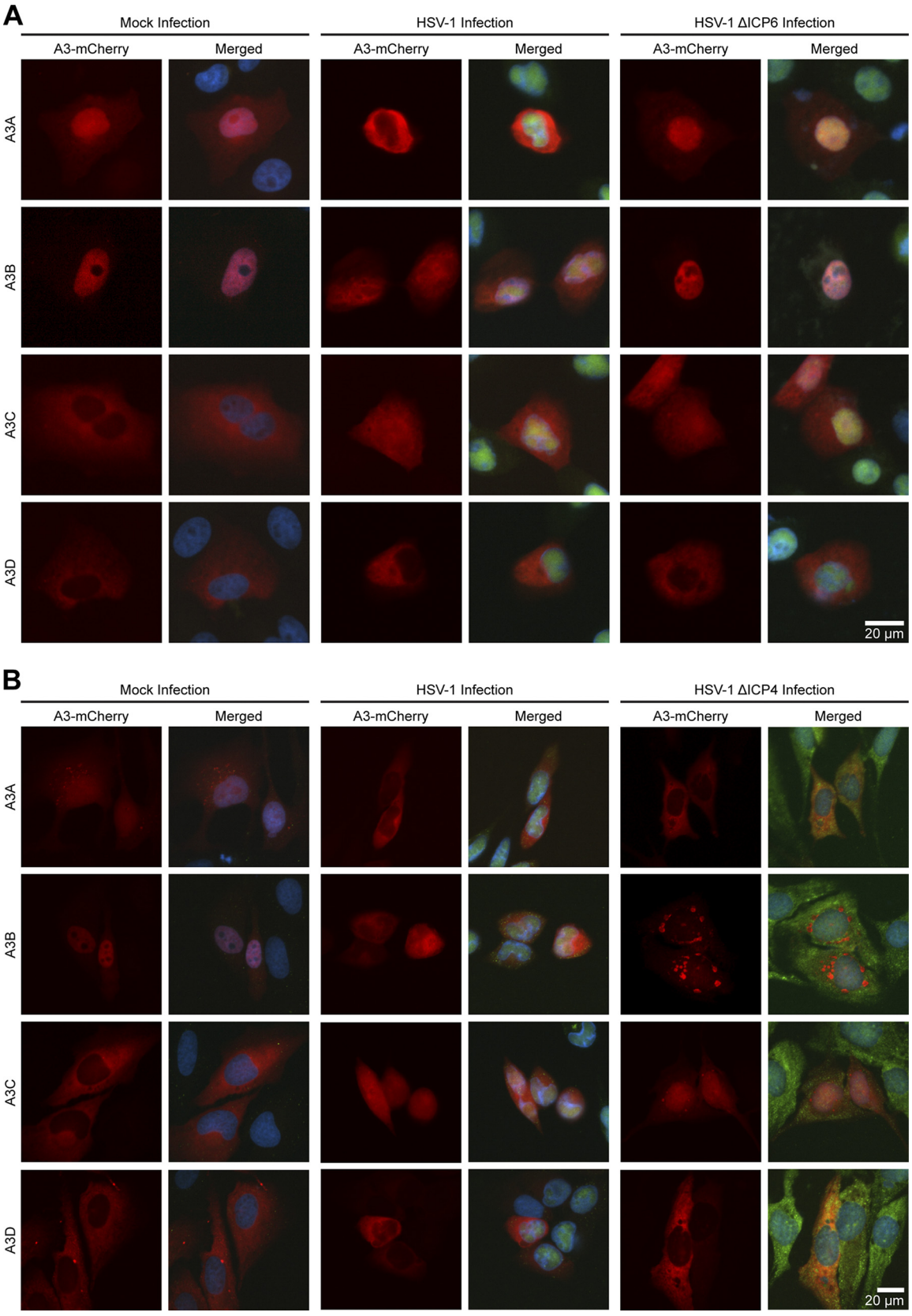

FIG 7 A3B and A3A relocalization is dependent on HSV-1 ICP6. (A) Representative images of Vero cells transfected with A3-mCherry constructs, followed by mock, wild-type HSV-1 KOS1.1, or HSV-1 KOS1.1ΔICP6 infection at 48 h posttransfection. Cells were fixed 8 h after HSV-1 infection, permeabilized, and stained with anti-ICP27 antibody to mark infected cells and Hoechst stain. (B) Representative images from an experiment similar to that described above for panel A, except using U2OS cells and the mutant virus HSV-1 KOS1.1ΔICP4.

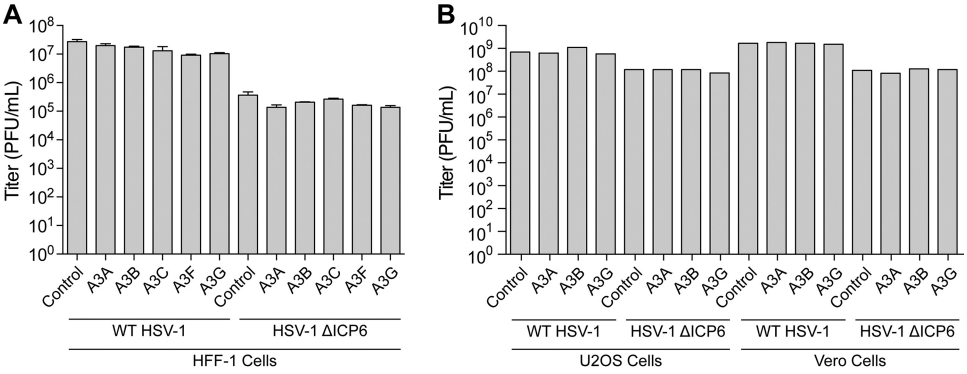

FIG 8 A3B and A3A do not impact HSV-1 replication or plaque formation. (A) Bar plot of HSV-1 titers produced from HFF-1 cells stably transduced with the control vector or the indicated HA-tagged A3 constructs. Cells were infected in triplicate at an MOI of 0.002 PFU/cell with either HSV-1 KOS1.1 or KOSΔICP6. The infected cultures were harvested at 48 hpi, and titers were determined on Vero cells to determine the level of viral progeny production. Statistical analysis was performed using unpaired Student's *t* test (n.s., not significant [$P > 0.01$ for all comparisons]). (B) Bar plot of KOS1.1 or KOSΔICP6 mutant stock titers determined on U2OS or Vero cells stably transduced with the control vector or the indicated HA-tagged A3 constructs. The cells were fixed at 72 hpi and stained with Giemsa stain for counting. WT, wild type.

The gamma- and alphaherpesvirus subfamilies encode both large and small RNR subunits (Fig. 1A). These RNRs are thought to serve the canonical function of synthesizing deoxyribonucleotides by reducing the 2′-hydroxyl from ribonucleotide substrates (31). While RNRs are essential for all cellular life, the requirement for endogenous viral RNRs differs tremendously across viral families. For example, most small double-stranded DNA (dsDNA) viruses and single-stranded DNA viruses do not encode RNRs and instead rely on host-encoded RNRs for deoxyribonucleotide production (32, 33). On the other hand, RNRs are almost ubiquitous among large dsDNA viruses, such as herpesviruses and poxviruses, presumably due to high deoxynucleoside triphosphate (dNTP) requirements during DNA replication (34–36). Betaherpesviruses such as CMV are an exception, however, because they lack a small subunit, and the large subunit has a defective catalytic site (37). In addition to ribonucleotide reductase activity, some viral RNRs have been shown to engage in noncatalytic activities that result in proviral phenotypes. For instance, the HSV-1 and HSV-2 large ribonucleotide reductase subunits, ICP6 and ICP10, respectively, have unique N-terminal extensions that block caspase-8 activity to inhibit apoptosis and bind RIP3 to promote necroptosis (38–41) (Fig. 1B). CMV UL45 also has antiapoptotic and pronecroptotic functions, suggesting that this could be its predominant function (41–43).

The answer to the question of whether A3B, A3A, or both enzymes are most relevant to gamma- and alphaherpesvirus pathogenesis is likely to depend, at least in part, on the complex interplay between viral tropism(s) and alternating modes of latent versus lytic replication. For EBV, epithelial cells serve as the source of primary infection, which are mandatory for establishing lytic replication cycles for person-to-person spread and enabling secondary infection of B lymphocytes for establishment of long-term latency (44). B cells also support lytic reactivation for reinfection and maintenance of EBV in the blood (45). Here, A3B may be more important than A3A simply because its expression is well documented in these cell types (46, 47). Likewise, KSHV infects epithelial and B cells but also engages in infection of clinically relevant endothelial cells, which can lead to Kaposi's sarcoma (48). Additionally, because monocytes are likely to be a secondary reservoir for KSHV infection (49–51), it is plausible that this virus requires the capacity to relocalize both A3B and A3A (A3B neutralization for replication in B cells and A3A neutralization for replication in monocytes/macrophages, where A3A is interferon inducible and capable of being expressed at extremely high levels [46, 52, 53]). For HSV-1, although neither A3B nor A3A expression has been reported in neural/central nervous system (CNS) cells, lytic replication in epithelial cells may require functional neutralization of A3B and/or A3A (54, 55).

The observation that the HSV-1 ΔICP6 mutant replicates at levels similar to those of wild-type HSV-1 in the presence of A3B or A3A was unexpected but not entirely surprising. Given the large genomes of herpesviruses, it is possible that other viral proteins may have overlapping redundant functions in A3 counteraction and/or repair mechanisms to overcome A3-mediated hypermutation. One prime candidate is the virally encoded uracil DNA glycosylase (UDG), encoded by the *UL2* gene, which has been shown to associate with the HSV-1 DNA polymerase in the infected cell nucleus (56). Consistent with this idea, we previously found that inhibition of the EBV UDG through expression of a universal UDG inhibitor (Ugi) results in enhanced A3B-mediated hypermutation of EBV genomes (18). It is thus possible that HSV-1 UL2 mediates the repair of uracil lesions generated by A3 enzymes, allowing the virus to tolerate moderate levels of mutation in the absence of ICP6. It is also conceivable that HSV-1 encodes an additional, novel A3A/B neutralization or escape mechanism that is able to fully compensate for the loss of ICP6 function (at least in the cell types tested here). Alternatively, inherent differences in viral DNA replication between HSV-1 and EBV could account for differences in replication phenotypes. HSV-1 replicates faster than EBV (57), which could result in less accessible single-stranded DNA for A3-mediated deamination. Finally, the lack of an *in vitro* infectivity phenotype does not preclude *in vivo* disease relevance. Although previous studies have tested the impact of A3A and A3G (and APOBEC1) on wild-type HSV-1 replication in transgenic mice (58, 59), dedicated functional studies with mutants that at least partly cripple each virus's A3 relocalization mechanism(s) in the most disease-relevant *in vivo* systems will be required to fully address the question of whether A3B, A3A, or both enzymes are relevant to the pathogenesis of these herpesviruses.

MATERIALS AND METHODS

Generation of a herpesvirus phylogenetic tree. Amino acid sequences for the following herpesvirus ribonucleotide reductase large subunits were obtained from the NCBI Protein RefSeq database: HSV-1 ICP6 (GenBank accession number YP_009137114.1), HSV-2 ICP10 (GenBank accession number YP_009137191.1), varicella-zoster virus (VZV) ORF19 (GenBank accession number NP_040142.1), EBV BORF2 (GenBank accession number YP_401655.1), human cytomegalovirus (HCMV) UL45 (GenBank accession number YP_081503.1), human herpesvirus 6A (HHV6A) U28 (GenBank accession number NP_042921.1), HHV6B U28 (GenBank accession number NP_050209.1), HHV7 U28 (GenBank accession number YP_073768.1), and KSHV ORF61 (GenBank accession number YP_001129418.1). The alignment was generated using MUSCLE (multiple-sequence alignment with high accuracy and high throughput) (60), and a phylogenetic tree was made using a neighbor-joining tree without distance corrections. The output was made using FigTree, using scaled branches (61).

DNA constructs for expression in human cell lines. The full set of pcDNA3.1(+) human APOBEC-HA expression constructs was described previously (62) (A3A [GenBank accession number NM_145699], A3B [GenBank accession number NM_004900], A3C [GenBank accession number NM_014508], A3D [GenBank accession number NM_152426], A3F [GenBank accession number NM_145298], A3G [GenBank accession number NM_021822], and A3H [haplotype II] [GenBank accession number FJ376615]). The full set of APOBEC-mCherry expression constructs was PCR amplified with Phusion high-fidelity DNA polymerase (catalogue number M0530; NEB) from previously described A3-mCherry constructs (22) and subcloned into pcDNA5/TO (catalogue number V103320; Invitrogen). The forward PCR primers are as follows: 5′-NNN NAA GCT TAC CAC CAT GGA AGC C-3′ for A3A, 5′-NNN NNA AGC TTA CCA CCA TGA ATC CA-3′ for A3B and A3C, 5′-NNN NNA AGC TTA CCA CCA TGA ATC CA-3′ for A3D, 5′-NNN NNA AGC TTA CCA CCA TGA AGC CT-3′ for A3F, 5′-NNN NAA GCT TAC CAC CAT GAA GCC T-3′ for A3G, and 5′-NNN NAA GCT TAC CAC CAT GGC TCT G-3′ for A3H. The reverse PCR primer used was 5′-AGA GTC GCG GCC GCT TAC TTG TAC A-3′. PCR fragments were digested with HindIII-HF (catalogue number R3104; NEB) and NotI-HF (catalogue number R3189; NEB) and ligated into pcDNA5/TO. The full set of pLenti-iA3i-HA constructs was previously described, except that the puromycin resistance gene was replaced with a hygromycin resistance gene (63). Briefly, this is a lentiviral construct with an intron spanning the A3 gene with a C-terminal 3×HA tag, arranged in the antisense direction, which is expressed after reverse transcription and integration. This construct bypasses the limitation of self-restriction by A3-mediated deamination of its own plasmid.

EBV BORF2 (GenBank accession number V01555.2) with a C-terminal 3×FLAG (DYKDDDDK) tag and EBV BaRF1 (GenBank accession number V01555.2) with a C-terminal 3×HA (YPYDVPDYA) tag were previously described (18). Other viral RNRs were subcloned with Phusion high-fidelity DNA polymerase from previously described pCMV-3F vectors (18).

KSHV ORF61 (GenBank accession number U75698.1) was PCR amplified using primers 5′-NNN NGA ATT CGC CAC CAT GTC TGT CCG GAC ATT TTG T-3′ and 5′-NNN NGA ATT CGC CAC CAT GTC TGT CCG GAC ATT TTG T-3′, digested with EcoRI-HF (catalogue number R3101S; NEB) and NotI-HF, and ligated into pcDNA4 with a C-terminal 3×FLAG tag. The same construct was PCR amplified using primers 5′-NNN

NGC GGC CGC GTC TGT CCG GAC ATT TTG T-3′ and 5′-NNN NTC TAG ATT ACT GAC AGA CCA GGC ACT C-3′, digested with NotI-HF and XbaI, and ligated into a similar pcDNA4 vector with an N-terminal 3×FLAG tag.

HSV-1 UL39 (GenBank accession number JN555585.1) was PCR amplified using primers 5′-NNN NGA TAT CCG CCA CCA TGG CCA GCC GCC CAG CC-3′ and 5′-NNN NGC GGC CGC CCC AGC GCG CAG CT-3′, digested with EcoRV-HF (catalogue number R1395; NEB) and NotI-HF, and ligated into pcDNA4 (catalogue number V102020; Invitrogen) with a C-terminal 3×FLAG tag (20). The same construct was PCR amplified using primers 5′-NNN NGC GGC CGC GGC CAG CCG CCC AGC CGC A-3′ and 5′-NNN NTC TAG ATT ACA GCG CGC AGC TCG TGC A-3′, digested with NotI-HF and XbaI (catalogue number R0145S; NEB), and ligated into a similar pcDNA4 vector with an N-terminal 3×FLAG tag.

Human cell culture. Unless indicated otherwise, cell lines were derived from established laboratory collections. All cell cultures were supplemented with 10% heat-inactivated fetal bovine serum (catalogue number 16140-063; Gibco) and 1× penicillin-streptomycin (catalogue number 15140122; Thermo Fisher) and periodically tested for mycoplasma (MycoAlert Plus, catalogue number LT07-710; Lonza). No cell lines have ever been mycoplasma positive or previously treated. 293T, Vero, and HFF-1 cells were cultured in high-glucose Dulbecco's modified Eagle's medium (DMEM) (HyClone), U2OS cells were cultured in McCoy's 5A medium (HyClone), and HeLa cells were cultured in RPMI 1640 (Corning).

Coimmunoprecipitation experiments and immunoblotting. Semiconfluent 293T cells were grown in 6-well plates and transfected with plasmids and 0.6 μl TransIT-LT1 (catalogue number 2304; Mirus) per 100 ng DNA in 100 μl serum-free Opti-MEM (catalogue number 31985062; Thermo Fisher). A titration series was performed to achieve roughly equivalent protein expression levels by immunoblotting for the A3 panel and RNR homologue in co-IP experiments. Growth medium was removed after 48 h, and whole cells were harvested in 1 ml phosphate-buffered saline (PBS)-EDTA by pipetting. Cells were spun down, PBS-EDTA was removed, and cells were resuspended in 300 μl of ice-cold lysis buffer (150 mM NaCl, 50 mM Tris-HCl, 10% glycerol, 1% IGEPAL [catalogue number I8896; Sigma], and a cOmplete EDTA-free protease inhibitor cocktail tablet [catalogue number 5056489001; Roche] [pH 7.4]). Cells were vortexed vigorously, left on ice for 30 min, and then sonicated for 5 s in an ice water bath. Thirty microliters of the whole-cell lysate was aliquoted for immunoblotting. Lysed cells were spun down at 13,000 rpm for 15 min to pellet debris, and the supernatant was added to a clean tube with 25 μl resuspended anti-FLAG M2 magnetic beads (catalogue number M8823; Sigma) for overnight incubation at 4°C with gentle rotation. Beads were then washed three times in 700 μl of ice-cold lysis buffer. Bound protein was eluted in 30 μl of elution butter (0.15 mg/ml 3×FLAG peptide [catalogue number F4799; Sigma] in 150 mM NaCl, 50 mM Tris-HCl, 10% glycerol, and 0.05% Tergitol [pH 7.4]). Proteins were analyzed by immunoblotting, and antibodies used included mouse anti-FLAG (1:5,000) (catalogue number F1804; Sigma), mouse antitubulin (1:10,000) (catalogue number T5168; Sigma), and rabbit anti-HA (1:3,000) (catalogue number C29F4; Cell Signaling).

HSV-1 infections and plaque assays. The HSV-1 strains used were wild-type strain KOS1.1 (64), K26GFP (27), the ICP6 deletion mutant ICP6Δ (28), and the ICP4 deletion mutant d120 (29). Titers of viral stocks were determined by plaque assays on either Vero cells (KOS1.1, K26GFP, and ICP6Δ) or ICP4-complemented E5-Vero cells (65). HSV-1 infections were carried out as described previously (66). For microscopy experiments, cells were infected at an MOI of 5 PFU/cell. To assay HSV-1 replication in A3-transduced HFF-1 cells, cells were infected at an MOI of 0.001 PFU/cell and incubated for 48 h, at which time a volume of sterilized milk equal to the volume of infected cell medium was added to each well, and the cells were frozen at −80°C. Infectious progeny virus was released by 3 cycles of freeze-thawing, and the titer was determined on Vero cells. HSV-1 plaque assays were carried out in liquid medium supplemented with 1% pooled normal human serum as previously described (66). For the HSV-1 plaque assays, U2OS or Vero cells were stably transduced with A3 constructs prior to carrying out plaque assays.

IF microscopy. For IF imaging of transfected cells, approximately 5×10^4 Vero, HeLa, or U2OS cells were plated on coverslips and, after 24 h, transfected with 200 ng pcDNA4-RNR-3×FLAG, 200 ng pcDNA5/TO-A3-mCherry, or both. After 48 h, cells were fixed in 4% formaldehyde, permeabilized in 0.2% Triton X-100 in PBS for 10 min, washed three times for 5 min in PBS, and incubated in blocking buffer (0.0028 M KH_2PO_4, 0.0072 M K_2HPO_4, 5% goat serum [Gibco], 5% glycerol, 1% cold water fish gelatin [Sigma], 0.04% sodium azide [pH 7.2]) for 1 h. Cells were then incubated in blocking buffer with primary mouse anti-FLAG (1:1,000) overnight at 4°C to detect FLAG-tagged RNRs. Cells were washed 3 times for 5 min with PBS and then incubated with the secondary antibody goat anti-mouse Alexa Fluor 488 (1:1,000) (catalogue number A11001; Invitrogen) diluted in blocking buffer for 2 h at room temperature in the dark. Cells were then counterstained with 1 μg/ml Hoechst 33342 for 10 min and rinsed twice for 5 min in PBS and once in sterile water. Coverslips were mounted on precleaned slides (Gold Seal Rite-On) using 20 to 30 μl of mounting medium (dissolved with 1 g *n*-propyl gallate [Sigma] in 40 ml glycerol and then pH adjusted to 8 to 8.5 by adding 0.35 ml of 0.1 M KH_2PO_4 and water to a final volume of 50 ml). Slides were imaged on a Nikon inverted Ti-E deconvolution microscope instrument and analyzed using NiS Elements.

For immunofluorescence imaging of HSV-1-infected cells, approximately 5×10^4 Vero, HeLa, or U2OS cells were plated on coverslips and, after 24 h, transfected with 200 ng pcDNA5/TO-A3-mCherry. After 48 h, cells were infected with HSV-1 K26GFP, HSV-1 KOS1.1, HSV-1 KOS1.1ΔICP6, or HSV-1 KOS1.1ΔICP4 at an MOI of 5. Cells were fixed in 4% formaldehyde at 8 h postinfection, and IF studies were then performed as described above. Time course experiments were fixed at either 3, 6, 9, or 12 h postinfection. HSV-1 K26GFP experiments did not require primary or secondary antibody staining steps. Cells infected with HSV-1 KOS1.1 and mutants were incubated with the primary antibody mouse anti-HSV-1 ICP27

H1113 (catalogue number sc69807; Santa Cruz) (1:1,000) overnight at 4°C to detect HSV-1-infected cells. Secondary antibody staining, counterstaining with Hoechst stain, mounting, and imaging were performed as described above.

IF microscopy quantification. For quantification of the ratio of nuclear/cytoplasmic A3, IF images were analyzed using Fiji software to obtain mean fluorescence intensities (MFIs) of nuclear compartments, determined by Hoechst stain outlines, and cytoplasmic compartments, determined by cell outlines. MFI values for each compartment were divided and plotted using Prism. Statistical analyses were performed using unpaired Student's *t* test.

ACKNOWLEDGMENTS

We thank Sandy Weller, Neal Deluca, and Prashant Desai for HSV-1 strains; M. Sanders and staff at the University of Minnesota Imaging Center for assistance with fluorescence microscopy; J. Becker for assistance with confocal microscopy; D. Ebrahimi for bioinformatics analyses of A3 expression in different cell types; and P. Southern for thoughtful comments and feedback on the manuscript.

These studies were supported in part by NCI grant P01 CA234228 and funds from the University of Minnesota College of Biological Sciences and Academic Health Center (to R.S.H.) as well as Canadian Institutes of Health Research (CIHR) project grant 153014 (to L.F.). NIH training grants provided salary support for A.Z.C. (F30 CA200432 and T32 GM008244) and M.C.J. (T32 CA009138). J.Y.-M. was supported by the Secretaría Nacional de Educación Superior, Ciencia, Tecnología e Innovación (SENESCYT). G.G. is a scholar under the Horizon2020 program (H2020 MSCA-ITN-2015). V.D.O. is supported by research grants from the University of Turin (RILO18) and from the Italian Ministry of Education, University and Research (MIUR) (PRIN 2015 and 2015RMNSTA). R.S.H. is the Margaret Harvey Schering Land Grant Chair for Cancer Research, a Distinguished McKnight University Professor, and an Investigator of the Howard Hughes Medical Institute. The funders had no role in study design, data collection and analysis, decision to publish, or preparation of the manuscript.

R.S.H. is a cofounder, shareholder, and consultant of ApoGen Biotechnologies Inc. The other authors have declared that no competing interests exist.

REFERENCES

1. Simon V, Bloch N, Landau NR. 2015. Intrinsic host restrictions to HIV-1 and mechanisms of viral escape. Nat Immunol 16:546–553. https://doi.org/10.1038/ni.3156.
2. Harris RS, Dudley JP. 2015. APOBECs and virus restriction. Virology 479–480:131–145. https://doi.org/10.1016/j.virol.2015.03.012.
3. Malim MH, Emerman M. 2008. HIV-1 accessory proteins—ensuring viral survival in a hostile environment. Cell Host Microbe 3:388–398. https://doi.org/10.1016/j.chom.2008.04.008.
4. Sheehy AM, Gaddis NC, Choi JD, Malim MH. 2002. Isolation of a human gene that inhibits HIV-1 infection and is suppressed by the viral Vif protein. Nature 418:646–650. https://doi.org/10.1038/nature00939.
5. Harris RS, Bishop KN, Sheehy AM, Craig HM, Petersen-Mahrt SK, Watt IN, Neuberger MS, Malim MH. 2003. DNA deamination mediates innate immunity to retroviral infection. Cell 113:803–809. https://doi.org/10.1016/s0092-8674(03)00423-9.
6. Wiegand HL, Doehle BP, Bogerd HP, Cullen BR. 2004. A second human antiretroviral factor, APOBEC3F, is suppressed by the HIV-1 and HIV-2 Vif proteins. EMBO J 23:2451–2458. https://doi.org/10.1038/sj.emboj.7600246.
7. Sasada A, Takaori-Kondo A, Shirakawa K, Kobayashi M, Abudu A, Hishizawa M, Imada K, Tanaka Y, Uchiyama T. 2005. APOBEC3G targets human T-cell leukemia virus type 1. Retrovirology 2:32. https://doi.org/10.1186/1742-4690-2-32.
8. Dang Y, Wang X, Esselman WJ, Zheng YH. 2006. Identification of APOBEC3DE as another antiretroviral factor from the human APOBEC family. J Virol 80:10522–10533. https://doi.org/10.1128/JVI.01123-06.
9. Esnault C, Heidmann O, Delebecque F, Dewannieux M, Ribet D, Hance AJ, Heidmann T, Schwartz O. 2005. APOBEC3G cytidine deaminase inhibits retrotransposition of endogenous retroviruses. Nature 433:430–433. https://doi.org/10.1038/nature03238.
10. Lee YN, Malim MH, Bieniasz PD. 2008. Hypermutation of an ancient human retrovirus by APOBEC3G. J Virol 82:8762–8770. https://doi.org/10.1128/JVI.00751-08.
11. Turelli P, Mangeat B, Jost S, Vianin S, Trono D. 2004. Inhibition of hepatitis B virus replication by APOBEC3G. Science 303:1829. https://doi.org/10.1126/science.1092066.
12. Suspene R, Guetard D, Henry M, Sommer P, Wain-Hobson S, Vartanian JP. 2005. Extensive editing of both hepatitis B virus DNA strands by APOBEC3 cytidine deaminases in vitro and in vivo. Proc Natl Acad Sci U S A 102:8321–8326. https://doi.org/10.1073/pnas.0408223102.
13. Vieira VC, Leonard B, White EA, Starrett GJ, Temiz NA, Lorenz LD, Lee D, Soares MA, Lambert PF, Howley PM, Harris RS. 2014. Human papillomavirus E6 triggers upregulation of the antiviral and cancer genomic DNA deaminase APOBEC3B. mBio 5:e02234-14. https://doi.org/10.1128/mBio.02234-14.
14. Vartanian JP, Guetard D, Henry M, Wain-Hobson S. 2008. Evidence for editing of human papillomavirus DNA by APOBEC3 in benign and precancerous lesions. Science 320:230–233. https://doi.org/10.1126/science.1153201.
15. Peretti A, Geoghegan EM, Pastrana DV, Smola S, Feld P, Sauter M, Lohse S, Ramesh M, Lim ES, Wang D, Borgogna C, FitzGerald PC, Bliskovsky V, Starrett GJ, Law EK, Harris RS, Killian JK, Zhu J, Pineda M, Meltzer PS, Boldorini R, Gariglio M, Buck CB. 2018. Characterization of BK polyomaviruses from kidney transplant recipients suggests a role for APOBEC3 in driving in-host virus evolution. Cell Host Microbe 23:628–635.e1–e7. https://doi.org/10.1016/j.chom.2018.04.005.
16. Verhalen B, Starrett GJ, Harris RS, Jiang M. 2016. Functional upregulation of the DNA cytosine deaminase APOBEC3B by polyomaviruses. J Virol 90:6379–6386. https://doi.org/10.1128/JVI.00771-16.
17. Narvaiza I, Linfesty DC, Greener BN, Hakata Y, Pintel DJ, Logue E, Landau NR, Weitzman MD. 2009. Deaminase-independent inhibition of parvoviruses by the APOBEC3A cytidine deaminase. PLoS Pathog 5:e1000439. https://doi.org/10.1371/journal.ppat.1000439.
18. Cheng AZ, Yockteng-Melgar J, Jarvis MC, Malik-Soni N, Borozan I, Carpenter MA, McCann JL, Ebrahimi D, Shaban NM, Marcon E, Greenblatt J,

Brown WL, Frappier L, Harris RS. 2019. Epstein-Barr virus BORF2 inhibits cellular APOBEC3B to preserve viral genome integrity. Nat Microbiol 4:78–88. https://doi.org/10.1038/s41564-018-0284-6.
19. Martinez T, Shapiro M, Bhaduri-McIntosh S, MacCarthy T. 2019. Evolutionary effects of the AID/APOBEC family of mutagenic enzymes on human gamma-herpesviruses. Virus Evol 5:vey040. https://doi.org/10.1093/ve/vey040.
20. Jager S, Kim DY, Hultquist JF, Shindo K, LaRue RS, Kwon E, Li M, Anderson BD, Yen L, Stanley D, Mahon C, Kane J, Franks-Skiba K, Cimermancic P, Burlingame A, Sali A, Craik CS, Harris RS, Gross JD, Krogan NJ. 2011. Vif hijacks CBF-beta to degrade APOBEC3G and promote HIV-1 infection. Nature 481:371–375. https://doi.org/10.1038/nature10693.
21. Zhang W, Du J, Evans SL, Yu Y, Yu XF. 2011. T-cell differentiation factor CBF-beta regulates HIV-1 Vif-mediated evasion of host restriction. Nature 481:376–379. https://doi.org/10.1038/nature10718.
22. Lackey L, Law EK, Brown WL, Harris RS. 2013. Subcellular localization of the APOBEC3 proteins during mitosis and implications for genomic DNA deamination. Cell Cycle 12:762–772. https://doi.org/10.4161/cc.23713.
23. Salamango DJ, McCann JL, Demir O, Brown WL, Amaro RE, Harris RS. 2018. APOBEC3B nuclear localization requires two distinct N-terminal domain surfaces. J Mol Biol 430:2695–2708. https://doi.org/10.1016/j.jmb.2018.04.044.
24. Salamango DJ, Becker JT, McCann JL, Cheng AZ, Demir O, Amaro RE, Brown WL, Shaban NM, Harris RS. 2018. APOBEC3H subcellular localization determinants define zipcode for targeting HIV-1 for restriction. Mol Cell Biol 38:e00356-18. https://doi.org/10.1128/MCB.00356-18.
25. Muckenfuss H, Hamdorf M, Held U, Perkovic M, Lower J, Cichutek K, Flory E, Schumann GG, Munk C. 2006. APOBEC3 proteins inhibit human LINE-1 retrotransposition. J Biol Chem 281:22161–22172. https://doi.org/10.1074/jbc.M601716200.
26. Bogerd HP, Wiegand HL, Hulme AE, Garcia-Perez JL, O'Shea KS, Moran JV, Cullen BR. 2006. Cellular inhibitors of long interspersed element 1 and Alu retrotransposition. Proc Natl Acad Sci U S A 103:8780–8785. https://doi.org/10.1073/pnas.0603313103.
27. Desai P, Person S. 1998. Incorporation of the green fluorescent protein into the herpes simplex virus type 1 capsid. J Virol 72:7563–7568.
28. Goldstein DJ, Weller SK. 1988. Factor(s) present in herpes simplex virus type 1-infected cells can compensate for the loss of the large subunit of the viral ribonucleotide reductase: characterization of an ICP6 deletion mutant. Virology 166:41–51. https://doi.org/10.1016/0042-6822(88)90144-4.
29. DeLuca NA, McCarthy AM, Schaffer PA. 1985. Isolation and characterization of deletion mutants of herpes simplex virus type 1 in the gene encoding immediate-early regulatory protein ICP4. J Virol 56:558–570.
30. Desai P, Ramakrishnan R, Lin ZW, Osak B, Glorioso JC, Levine M. 1993. The RR1 gene of herpes simplex virus type 1 is uniquely trans activated by ICP0 during infection. J Virol 67:6125–6135.
31. Torrents E. 2014. Ribonucleotide reductases: essential enzymes for bacterial life. Front Cell Infect Microbiol 4:52. https://doi.org/10.3389/fcimb.2014.00052.
32. Cohen D, Adamovich Y, Reuven N, Shaul Y. 2010. Hepatitis B virus activates deoxynucleotide synthesis in nondividing hepatocytes by targeting the R2 gene. Hepatology 51:1538–1546. https://doi.org/10.1002/hep.23519.
33. Kitab B, Satoh M, Ohmori Y, Munakata T, Sudoh M, Kohara M, Tsukiyama-Kohara K. 2019. Ribonucleotide reductase M2 promotes RNA replication of hepatitis C virus by protecting NS5B protein from hPLIC1-dependent proteasomal degradation. J Biol Chem 294:5759–5773. https://doi.org/10.1074/jbc.RA118.004397.
34. Iyer LM, Aravind L, Koonin EV. 2001. Common origin of four diverse families of large eukaryotic DNA viruses. J Virol 75:11720–11734. https://doi.org/10.1128/JVI.75.23.11720-11734.2001.
35. Sakowski EG, Munsell EV, Hyatt M, Kress W, Williamson SJ, Nasko DJ, Polson SW, Wommack KE. 2014. Ribonucleotide reductases reveal novel viral diversity and predict biological and ecological features of unknown marine viruses. Proc Natl Acad Sci U S A 111:15786–15791. https://doi.org/10.1073/pnas.1401322111.
36. Zhao Y, Temperton B, Thrash JC, Schwalbach MS, Vergin KL, Landry ZC, Ellisman M, Deerinck T, Sullivan MB, Giovannoni SJ. 2013. Abundant SAR11 viruses in the ocean. Nature 494:357–360. https://doi.org/10.1038/nature11921.
37. Lembo D, Brune W. 2009. Tinkering with a viral ribonucleotide reductase. Trends Biochem Sci 34:25–32. https://doi.org/10.1016/j.tibs.2008.09.008.
38. Langelier Y, Bergeron S, Chabaud S, Lippens J, Guilbault C, Sasseville AM, Denis S, Mosser DD, Massie B. 2002. The R1 subunit of herpes simplex virus ribonucleotide reductase protects cells against apoptosis at, or upstream of, caspase-8 activation. J Gen Virol 83:2779–2789. https://doi.org/10.1099/0022-1317-83-11-2779.
39. Dufour F, Sasseville AM, Chabaud S, Massie B, Siegel RM, Langelier Y. 2011. The ribonucleotide reductase R1 subunits of herpes simplex virus types 1 and 2 protect cells against TNFalpha- and FasL-induced apoptosis by interacting with caspase-8. Apoptosis 16:256–271. https://doi.org/10.1007/s10495-010-0560-2.
40. Huang Z, Wu SQ, Liang Y, Zhou X, Chen W, Li L, Wu J, Zhuang Q, Chen C, Li J, Zhong CQ, Xia W, Zhou R, Zheng C, Han J. 2015. RIP1/RIP3 binding to HSV-1 ICP6 initiates necroptosis to restrict virus propagation in mice. Cell Host Microbe 17:229–242. https://doi.org/10.1016/j.chom.2015.01.002.
41. Mocarski ES, Guo H, Kaiser WJ. 2015. Necroptosis: the Trojan horse in cell autonomous antiviral host defense. Virology 479–480:160–166. https://doi.org/10.1016/j.virol.2015.03.016.
42. Kwon KM, Oh SE, Kim YE, Han TH, Ahn JH. 2017. Cooperative inhibition of RIP1-mediated NF-kappaB signaling by cytomegalovirus-encoded deubiquitinase and inactive homolog of cellular ribonucleotide reductase large subunit. PLoS Pathog 13:e1006423. https://doi.org/10.1371/journal.ppat.1006423.
43. Mack C, Sickmann A, Lembo D, Brune W. 2008. Inhibition of proinflammatory and innate immune signaling pathways by a cytomegalovirus RIP1-interacting protein. Proc Natl Acad Sci U S A 105:3094–3099. https://doi.org/10.1073/pnas.0800168105.
44. Sitki-Green D, Covington M, Raab-Traub N. 2003. Compartmentalization and transmission of multiple Epstein-Barr virus strains in asymptomatic carriers. J Virol 77:1840–1847. https://doi.org/10.1128/jvi.77.3.1840-1847.2003.
45. Kenney SC, Mertz JE. 2014. Regulation of the latent-lytic switch in Epstein-Barr virus. Semin Cancer Biol 26:60–68. https://doi.org/10.1016/j.semcancer.2014.01.002.
46. Koning FA, Newman EN, Kim EY, Kunstman KJ, Wolinsky SM, Malim MH. 2009. Defining APOBEC3 expression patterns in human tissues and hematopoietic cell subsets. J Virol 83:9474–9485. https://doi.org/10.1128/JVI.01089-09.
47. Burns MB, Lackey L, Carpenter MA, Rathore A, Land AM, Leonard B, Refsland EW, Kotandeniya D, Tretyakova N, Nikas JB, Yee D, Temiz NA, Donohue DE, McDougle RM, Brown WL, Law EK, Harris RS. 2013. APOBEC3B is an enzymatic source of mutation in breast cancer. Nature 494:366–370. https://doi.org/10.1038/nature11881.
48. Chakraborty S, Veettil MV, Chandran B. 2012. Kaposi's sarcoma associated herpesvirus entry into target cells. Front Microbiol 3:6. https://doi.org/10.3389/fmicb.2012.00006.
49. Blasig C, Zietz C, Haar B, Neipel F, Esser S, Brockmeyer NH, Tschachler E, Colombini S, Ensoli B, Sturzl M. 1997. Monocytes in Kaposi's sarcoma lesions are productively infected by human herpesvirus 8. J Virol 71:7963–7968.
50. Wu W, Vieira J, Fiore N, Banerjee P, Sieburg M, Rochford R, Harrington W, Jr, Feuer G. 2006. KSHV/HHV-8 infection of human hematopoietic progenitor (CD34+) cells: persistence of infection during hematopoiesis in vitro and in vivo. Blood 108:141–151. https://doi.org/10.1182/blood-2005-04-1697.
51. Kim IJ, Flano E, Woodland DL, Lund FE, Randall TD, Blackman MA. 2003. Maintenance of long term gamma-herpesvirus B cell latency is dependent on CD40-mediated development of memory B cells. J Immunol 171:886–892. https://doi.org/10.4049/jimmunol.171.2.886.
52. Stenglein MD, Burns MB, Li M, Lengyel J, Harris RS. 2010. APOBEC3 proteins mediate the clearance of foreign DNA from human cells. Nat Struct Mol Biol 17:222–229. https://doi.org/10.1038/nsmb.1744.
53. Thielen BK, McNevin JP, McElrath MJ, Hunt BV, Klein KC, Lingappa JR. 2010. Innate immune signaling induces high levels of TC-specific deaminase activity in primary monocyte-derived cells through expression of APOBEC3A isoforms. J Biol Chem 285:27753–27766. https://doi.org/10.1074/jbc.M110.102822.
54. Nicoll MP, Proenca JT, Efstathiou S. 2012. The molecular basis of herpes simplex virus latency. FEMS Microbiol Rev 36:684–705. https://doi.org/10.1111/j.1574-6976.2011.00320.x.
55. Akhtar J, Shukla D. 2009. Viral entry mechanisms: cellular and viral mediators of herpes simplex virus entry. FEBS J 276:7228–7236. https://doi.org/10.1111/j.1742-4658.2009.07402.x.
56. Bogani F, Corredeira I, Fernandez V, Sattler U, Rutvisuttinunt W, Defais M, Boehmer PE. 2010. Association between the herpes simplex virus-1 DNA

polymerase and uracil DNA glycosylase. J Biol Chem 285:27664–27672. https://doi.org/10.1074/jbc.M110.131235.
57. Baron S (ed). 1996. Medical microbiology, 4th ed. University of Texas Medical Branch at Galveston, Galveston, TX.
58. Nakaya Y, Stavrou S, Blouch K, Tattersall P, Ross SR. 2016. In vivo examination of mouse APOBEC3- and human APOBEC3A- and APOBEC3G-mediated restriction of parvovirus and herpesvirus infection in mouse models. J Virol 90:8005–8012. https://doi.org/10.1128/JVI.00973-16.
59. Gee P, Ando Y, Kitayama H, Yamamoto SP, Kanemura Y, Ebina H, Kawaguchi Y, Koyanagi Y. 2011. APOBEC1-mediated editing and attenuation of herpes simplex virus 1 DNA indicate that neurons have an antiviral role during herpes simplex encephalitis. J Virol 85:9726–9736. https://doi.org/10.1128/JVI.05288-11.
60. Edgar RC. 2004. MUSCLE: multiple sequence alignment with high accuracy and high throughput. Nucleic Acids Res 32:1792–1797. https://doi.org/10.1093/nar/gkh340.
61. Bouckaert R, Heled J, Kuhnert D, Vaughan T, Wu CH, Xie D, Suchard MA, Rambaut A, Drummond AJ. 2014. BEAST 2: a software platform for Bayesian evolutionary analysis. PLoS Comput Biol 10:e1003537. https://doi.org/10.1371/journal.pcbi.1003537.
62. Larue RS, Lengyel J, Jonsson SR, Andresdottir V, Harris RS. 2010. Lentiviral Vif degrades the APOBEC3Z3/APOBEC3H protein of its mammalian host and is capable of cross-species activity. J Virol 84:8193–8201. https://doi.org/10.1128/JVI.00685-10.
63. Law EK, Sieuwerts AM, LaPara K, Leonard B, Starrett GJ, Molan AM, Temiz NA, Vogel RI, Meijer-van Gelder ME, Sweep FC, Span PN, Foekens JA, Martens JW, Yee D, Harris RS. 2016. The DNA cytosine deaminase APOBEC3B promotes tamoxifen resistance in ER-positive breast cancer. Sci Adv 2:e1601737. https://doi.org/10.1126/sciadv.1601737.
64. Hughes RG, Jr, Munyon WH. 1975. Temperature-sensitive mutants of herpes simplex virus type 1 defective in lysis but not in transformation. J Virol 16:275–283.
65. DeLuca NA, Schaffer PA. 1988. Physical and functional domains of the herpes simplex virus transcriptional regulatory protein ICP4. J Virol 62:732–743.
66. Park D, Lalli J, Sedlackova-Slavikova L, Rice SA. 2015. Functional comparison of herpes simplex virus 1 (HSV-1) and HSV-2 ICP27 homologs reveals a role for ICP27 in virion release. J Virol 89:2892–2905. https://doi.org/10.1128/JVI.02994-14.